Available online at www.sciencedirect.com
ScienceDirect
Catalysis Today 126 (2007) 112–118
CATALYSIS TODAY
www.elsevier.com/locate/cattod

Structure stabilizing effect of tungsten in mixed molybdenum oxides with Mo_5O_{14}-type structure

E. Rödel [a], O. Timpe [a], A. Trunschke [a], G.A. Zenkovets [b], G.N. Kryukova [b], R. Schlögl [a], T. Ressler [c,*]

[a] *Fritz-Haber-Institut der MPG, Department of Inorganic Chemistry, Faradayweg 4-6, D-14195 Berlin, Germany*
[b] *Boreskov Institute of Catalysis, Novosibirsk 630090, Russia*
[c] *Technische Universität Berlin, Institute of Chemistry, Sekr. C2, Strasse des 17. Juni 135, D-10623 Berlin, Germany*

Available online 16 May 2007

Abstract

Bulk structural properties of single phase crystalline $(Mo_{0.91}V_{0.09})_5O_{14}$ and $(Mo_{0.68}V_{0.23}W_{0.09})_5O_{14}$ materials were investigated using in situ X-ray diffraction and in situ X-ray absorption spectroscopy at three metal edges. Temperature programmed experiments in reducing (propene) and oxidizing (oxygen) atmosphere and isothermal redox experiments at 773 K revealed differences in the bulk properties of the two phases studied. A structure stabilizing effect of tungsten in $(MoVW)_5O_{14}$ under oxidizing conditions was found. Moreover, tungsten centers in a (MoVW) dioxide material exert a structure-directing effect towards re-oxidation to a Mo_5O_{14}-type structure.

Keywords: Mo_5O_{14}-type structure; X-ray diffraction; XAS; Redox properties

1. Introduction

Molybdenum containing metal oxide catalysts selectively oxidize propene to acrylic acid. The ability of molybdenum to occur in various coordination geometries gives rise to a high structural diversity of the mixed transition metal oxides. Catalytically active sites in these mixed oxides may be stabilized by characteristic structural motifs induced by the cationic composition [1,2]. Small amounts of V or W in Mo oxides may result in the formation of (MoV) oxides and (MoVW) oxides that crystallize in the tetragonal Mo_5O_{14} structure [3]. This structure has been suggested to represent the motif of the active phase for the selective oxidation of acrolein into acrylic acid [4,5]. The Mo_5O_{14} structure corresponds to a pentagonal column phase with a narrow phase width and an open structure with five- and six-fold channels parallel to the *c*-axis [6]. Several possible compositions with various cations stabilizing the Mo_5O_{14} structure have been described in the literature [7–13].

Here, $(MoVW)_5O_{14}$ and $(MoV)_5O_{14}$ have been prepared as crystalline single phase materials exhibiting catalytic activity in the selective oxidation of propene [14,24]. In situ X-ray diffraction (XRD) and in situ X-ray absorption spectroscopy (XAS) combined with online gas phase analysis are used to explore the structural evolution of these single phase Mo_5O_{14}-type materials under varying reactive atmospheres. XRD and XAS give access to both the long-range order of the materials and the local structure around the metal centers in these mixed oxides.

2. Experimental

2.1. Preparation

The precursor of the $(MoVW)_5O_{14}$ material was prepared as described previously [14]. Ammonium heptamolybdate (AHM) (c = 0.963 mol/L) and ammonium metatungstate (AMT) (c = 0.27 mol/L) were dissolved in bidistilled water at 353 K. V_2O_5 was dissolved in an aqueous solution of 1.93 mol/L oxalic acid at 353 K (vanadyl oxalate aqueous solution c = 0.379 mol/L). The solutions were mixed in a 2 L batch and heated to 353 K for 1 h. After spray-drying of the mixed solutions the resulting

* Corresponding author. Tel.: +49 30 8413 3192; fax: +49 30 314 21106.
E-mail addresses: Thorsten.Ressler@TU-berlin.de, ressler@fhi-berlin.mpg.de (T. Ressler).

0920-5861/$ – see front matter © 2007 Elsevier B.V. All rights reserved.
doi:10.1016/j.cattod.2007.03.004

material was calcined for 2 h in synthetic air at 623 K and then heated for 2 h in helium at 713 K. The metal content in the $(MoVW)_5O_{14}$ phase amounted to 68 mol% Mo, 23 mol% V, and 9 mol% W.

The $(MoV)_5O_{14}$ material was prepared as follows. An aqueous solution of vanadyl oxalate was obtained by dissolving 7.7 mg V_2O_5 and 15.9 mg oxalic acid in 132 mL water. The resulting blue solution was mixed with a solution of 200 mg AHM in 500 mL water at 353 K. After stirring at this temperature for 1 h, the solution was spray-dried. The spray-dried powder was treated in helium at 773 K for 4 h followed by dissolution of impurities in 1 mol/L ammonia solution at 313 K for 5 min. Subsequently, the resulting material was heated in helium to 773 K for 4 h. The metal content in the $(MoV)_5O_{14}$ phase amounted to 91 mol% Mo and 9 mol% V.

2.2. In situ X-ray diffraction

Combined in situ XRD/MS experiments were performed on a STOE Theta/Theta diffractometer (secondary Si(1 1 1) monochromator, Cu Kα radiation). About 30–80 mg of the powdered $(MoVW)_5O_{14}$ or $(MoV)_5O_{14}$ were used. The diffractometer was equipped with a XRK 900 high temperature cell from Anton Paar. All measurements were conducted under atmospheric pressure in flowing atmosphere at 100 mL/min. The gas phase composition at the cell outlet was analyzed on line with a mass spectrometer (Omnistar, QMS Pfeiffer). Ex situ XRD measurements were performed on a STOE STADI-P diffractometer with a Ge(1 1 1) primary monochromator and a position sensitive detector. Phase analysis was performed using the DIFFRAC PLUS evaluation software [15]. Structure refinement was conducted using the TOPAS 3 software package [16] and single crystal data taken from the inorganic crystal structure database (ICSD [17]).

2.3. In situ X-ray absorption spectroscopy

XAS measurements were performed in the transmission mode at the Mo K edge (19.999 keV), W L_{III} (10.204 keV) edge, and at the V K edge (5.465 keV) at beamline X1 and E4 at the Hamburger Synchrotronstrahlungslabor, HASYLAB, respectively. The experiments were conducted in a flow reactor of ∼4 mL volume at atmospheric pressure in 30 mL/min flowing reactants. The gas phase composition at the cell outlet was analyzed on line with a mass spectrometer (Omnistar, QMS Pfeiffer). About 30 mg BN were mixed with about 8 mg sample, ground, and pressed at a force of 1 tonne into a pellet of 5 mm in diameter. The resulting edge jump amounted to $\Delta\mu \sim 1$ at the Mo K edge, $\Delta\mu \sim 0.2$–0.3 at the V K edge, and $\Delta\mu \sim 0.8$ at the W L_{III} edge. Data processing and analysis was performed with the software package WinXAS 3.1 [18]. The photon energy was calibrated to a spectrum of the corresponding metal. First order polynomials were chosen for background subtraction. Third order (Mo K edge) or second order (V K edge, W L_{III} edge) polynomials were used for normalization. Average valences of vanadium were determined from the pre-edge peak height [19]. The average valence of molybdenum was obtained from analyzing the Mo K edge position according to a previously reported procedure [20].

2.4. Reduction and re-oxidation experiments

The structural evolution of $(MoVW)_5O_{14}$ and $(MoV)_5O_{14}$ was investigated during temperature-programmed and isothermal experiments. Temperature-programmed XAS and XRD measurements were conducted in reducing (10% propene) and oxidizing (20% oxygen) atmospheres in the temperature range from 300 to 773 K. A heating rate of 3 K/min (XAS) or 0.4 K/min (XRD, average heating rate) was used. Prior to the isothermal redox experiments, $(MoVW)_5O_{14}$ and $(MoV)_5O_{14}$ were heated in helium to 773 K at a heating rate of 10 K/min. The structural stability of the materials in helium at 773 K was confirmed by XRD and XAS. Subsequently, the atmosphere was switched to 10% propene or 10% hydrogen at 773 K and XRD or XAS scans were measured until the sample was completely reduced. The resulting materials were re-oxidized in 20% oxygen at 773 K and XRD or XAS scans were measured until complete re-oxidation. In addition, XRD and XAS scans were measured at 300 K before and after the temperature-programmed and isothermal experiments.

2.5. Catalytic properties

The structural evolution and catalytic properties of $(MoVW)_5O_{14}$ and $(MoV)_5O_{14}$ were investigated during in situ XRD and in situ XAS experiments in 5% propene and 10% oxygen from 300 to 773 K at a heating rate of 5 K/min (XAS) and 0.7 K/min (XRD, average heating rate). During in situ XAS measurements scans (5 min duration per scan) were taken during the heating ramp. During in situ XRD scans were taken in isothermal segments each 50 K. The formation of products was monitored by mass spectroscopy using a quadrupole mass spectrometer (Omnistar, QMS Pfeiffer).

3. Results

3.1. Characterization of $(MoVW)_5O_{14}$ and $(MoV)_5O_{14}$

Phase purity of the $(MoV)_5O_{14}$ and the $(MoVW)_5O_{14}$ materials used was verified by XRD [21]. Lattice constants obtained from the refinement of the tetragonal Mo_5O_{14} structure (ICSD [27202]) to the experimental XRD pattern are given in Table 1. No detectable amounts of amorphous materials were found in a XRD analysis of a mixture of 50% $(MoVW)_5O_{14}$ and 50% α-Al_2O_3 as internal standard. The characteristic XRD pattern of the Mo_5O_{14} structure are given in

Table 1
Lattice constants from XRD refinement of tetragonal $(MoVW)_5O_{14}$ and $(MoV)_5O_{14}$ based on ICSD [27202]

	$(MoV)_5O_{14}$	$(MoVW)_5O_{14}$
a (Å)	22.88	22.76
c (Å)	4.00	3.99

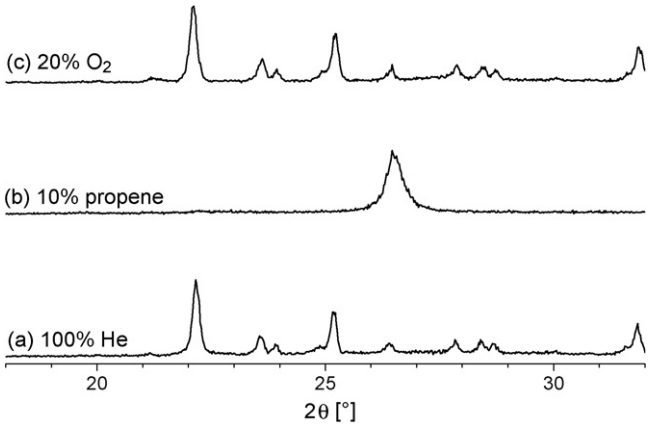

Fig. 1. In situ XRD of sample $(MoVW)_5O_{14}$ during redox experiment: (a) heating in helium to 773 K, (b) isothermal reduction at 773 K in 10% propene and (c) re-oxidation in 20% oxygen at 773 K.

Figs. 1a and 2a. Transmission electron microscopy investigations showed only the Mo_5O_{14}-type structures in $(MoVW)_5O_{14}$ and $(MoV)_5O_{14}$.

3.2. Redox properties of $(MoVW)_5O_{14}$ and $(MoV)_5O_{14}$

3.2.1. In situ X-ray diffraction

The Mo_5O_{14}-type structure of $(MoVW)_5O_{14}$ and $(MoV)_5O_{14}$ was stable during heating in helium to 773 K (Figs. 1a and 2a). Under reducing conditions in 10% propene at 773 K, the $(MoV)_5O_{14}$ and $(MoVW)_5O_{14}$ materials were completely transformed into monoclinic MoO_2-type structures (Figs. 1b and 2b). Lattice constants obtained from a refinement of a MoO_2 model structure (ICSD [23722]) to the patterns of the MoO_2-type phases are given in Table 2. Compared to the (MoVW) dioxide, the lattice constants of the (MoV) dioxide material that contains less vanadium showed an expansion of the *a*-axis, shortening of the *b*- and *c*-axis, and an increased unit cell volume. Upon switching to 20% oxygen at 773 K, the (MoVW) dioxide was re-oxidized and the resulting oxide exhibited the Mo_5O_{14}-type structure of the initial $(MoVW)_5O_{14}$

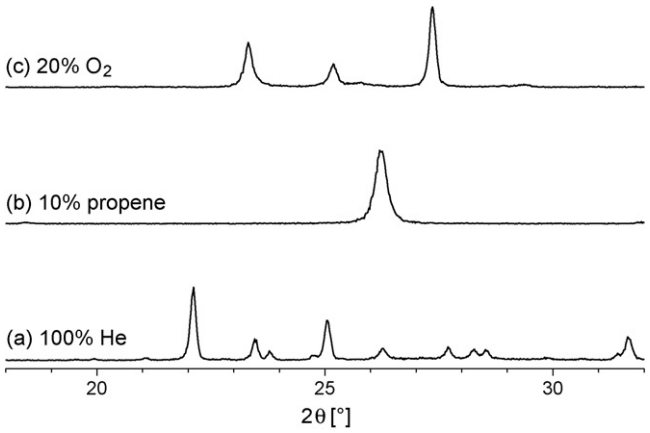

Fig. 2. In situ XRD of $(MoV)_5O_{14}$ during redox experiment: (a) heating in helium to 773 K, (b) isothermal reduction at 773 K in 10% propene and (c) re-oxidation in 20% oxygen at 773 K.

Table 2
Lattice constants from XRD refinement of monoclinic (MoVW) dioxide and (MoV) dioxide based on ICSD [23722]

	(MoV) dioxide	(MoVW) dioxide
a (Å)	5.69	5.63
b (Å)	4.79	4.84
c (Å)	5.56	5.61
β (°)	121.17	121.00

material (Fig. 1c). Conversely, re-oxidation of the (MoV) dioxide in 20% oxygen at 773 K resulted in an orthorhombic MoO_3-type structure (Fig. 2c). No intermediate Mo oxide phases were detectable in the XRD patterns during reduction and re-oxidation.

Temperature-programmed XRD measurements in 10% propene yielded an onset of reduction of the $(MoVW)_5O_{14}$ material to a monoclinic MoO_2-type structure at 723 K. Conversely, reduction of $(MoV)_5O_{14}$ to a monoclinic MoO_2-type structure started already at 673 K. During temperature programmed thermal treatment of $(MoVW)_5O_{14}$ in 20% oxygen, the Mo_5O_{14}-type structure was stable up to 773 K. No oxidation or decomposition was observed. Conversely, the Mo_5O_{14}-type structure of $(MoV)_5O_{14}$ was stable during treatment in 20% oxygen only below 723 K. Above 723 K the Mo_5O_{14}-type structure of $(MoV)_5O_{14}$ slowly decomposed and was oxidized into a MoO_3-type structure.

3.2.2. In situ XAS

Very similar Mo K near-edge spectra of $(MoVW)_5O_{14}$ and $(MoV)_5O_{14}$ are indicative of molybdenum centers in a similar local structural coordination in both materials. The same holds for the local structure around the V centers in $(MoVW)_5O_{14}$ and $(MoV)_5O_{14}$ (Fig. 3). Compared to the V K edge spectra of VO_2 and V_2O_5 references, the average valence of the V centers in $(MoVW)_5O_{14}$ and $(MoV)_5O_{14}$ amounts to about 4.5. Near-edge spectra at the Mo K, V K, and W L_{III} edges of the initial $(MoVW)_5O_{14}$ are shown in Fig. 4. Moreover, Fig. 4 depicts the near-edge spectra of the $(MoVW)_5O_{14}$ material obtained after a cycle of reduction in propene and re-oxidation at 773 K. Apparently, a similar local and electronic structure of all metal centers is found in the initial and the re-oxidized $(MoVW)_5O_{14}$ material. Conversely, the Mo K and V K near-edge spectra of the initial $(MoV)_5O_{14}$ and the re-oxidized material indicate a different local structure around the molybdenum and vanadium centers. Moreover, compared to the spectrum of a MoO_3 reference, the Mo centers in the MoO_3-type structure of the re-oxidized (MoV) oxide exhibit a slightly reduced average valence (∼5.8) and a different local structure. The latter maybe due to the incorporation of vanadium centers in the MoO_3-type structure. Furthermore, XRD analysis of the material obtained from re-oxidizing the (MoV) dioxide yielded a minor amount of a mixed $Mo_xV_{2-x}O_5$ phase (e.g. 0.5% $Mo_{0.56}V_{1.44}O_5$ ICSD [24338]).

Mo centers in the as-prepared $(MoVW)_5O_{14}$ and $(MoV)_5O_{14}$ materials exhibited an average valence of less than 6 (∼5.8). A similarly reduced average valence was observed for the Mo centers in the Mo_5O_{14}-type structure obtained from

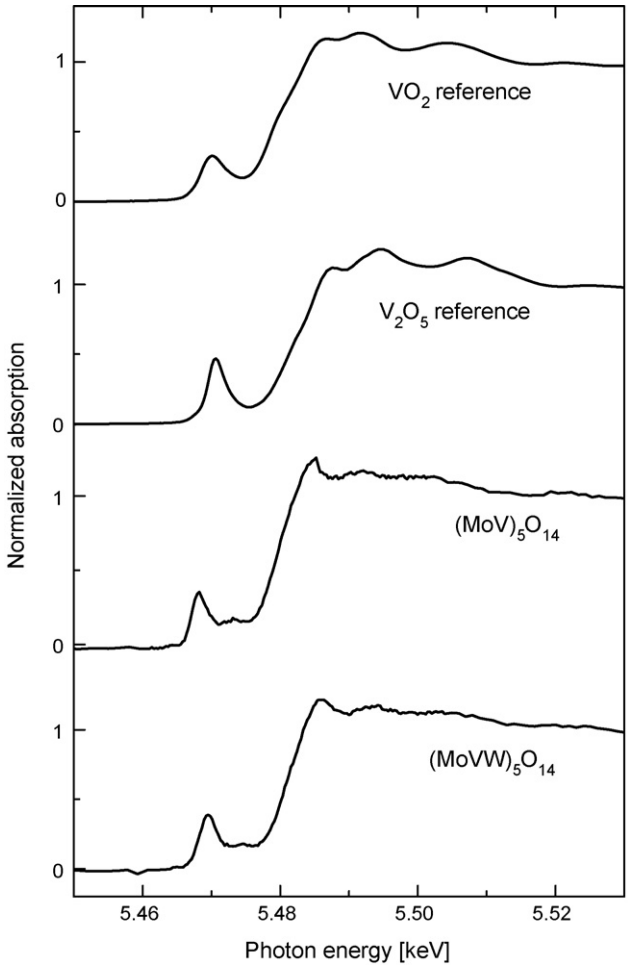

Fig. 3. XANES spectra taken at V K edge of the initial $(MoVW)_5O_{14}$ and $(MoV)_5O_{14}$ compared to references VO_2 and V_2O_5.

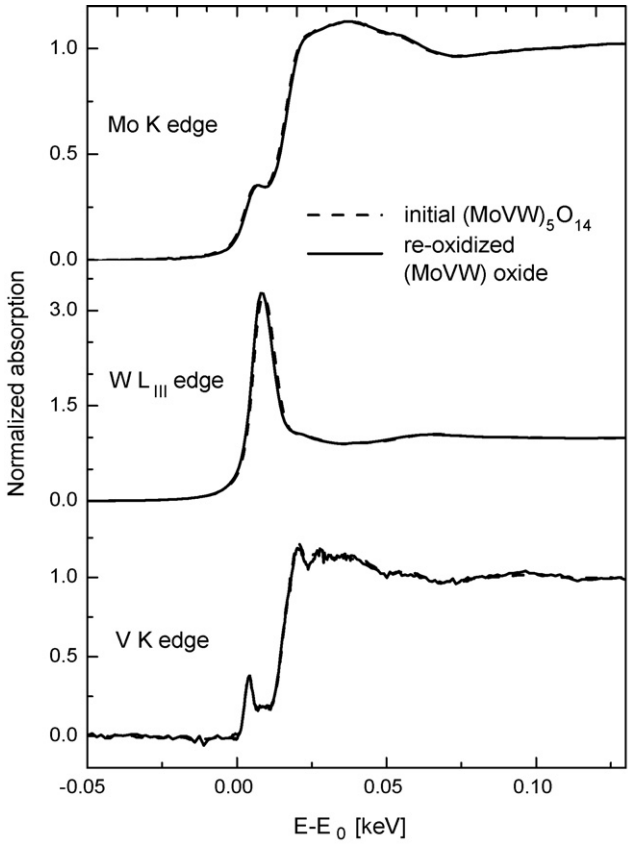

Fig. 4. XANES spectra measured at the Mo K edge, W L_{III} edge, and V K edge of initial $(MoVW)_5O_{14}$ and re-oxidized (MoVW) oxide.

re-oxidizing the (MoVW) dioxide. Conversely, the Mo centers in the MoO_3-type structure obtained from re-oxidizing the (MoV) dioxide exhibit an average valence of 5.8. The local structure and the average valence of the Mo centers in the (MoVW) dioxide and the (MoV) dioxide were similar to those of the Mo centers in MoO_2 (Fig. 5). Slight differences are indicative of the incorporation of V and W in the corresponding MoO_2-type structures. The V K near-edge spectra of the dioxides obtained from reducing the corresponding Mo_5O_{14}-type oxides in propene at 773 K are depicted in Fig. 6. Apparently, the average valance and the local structure of the V centers in the dioxide materials is similar to those of the V centers in V_2O_3.

Mo K near-edge spectra measured during temperature programmed treatment of $(MoVW)_5O_{14}$ and $(MoV)_5O_{14}$ in 10% propene showed an onset of transformation into a MoO_2-type structure at a temperature of ~685 K. Conversely, V K and W L_{III} near-edge spectra measured during treatment of $(MoVW)_5O_{14}$ and $(MoV)_5O_{14}$ in 10% propene exhibited an onset of structural changes at ~650 K. In particular, a decrease in the characteristic V K pre-edge peak height at ~650 K was observed. This is indicative of an onset of reduction of the V centers in the Mo_5O_{14}-type structures prior to a detectable reduction of the Mo centers. The detailed EXAFS analysis of the structural changes occurring during thermal treatment of the Mo_5O_{14}-type materials is underway.

3.2.3. Catalytic properties of $(MoVW)_5O_{14}$ and $(MoV)_5O_{14}$

During in situ XRD experiments of $(MoVW)_5O_{14}$ and $(MoV)_5O_{14}$ in 5% propene and 10% oxygen the long-range order of the Mo_5O_{14}-type structure did not change. Fig. 7 shows the lattice expansion of $(MoVW)_5O_{14}$ which is not linear with temperature but essentially occurs at temperatures higher than

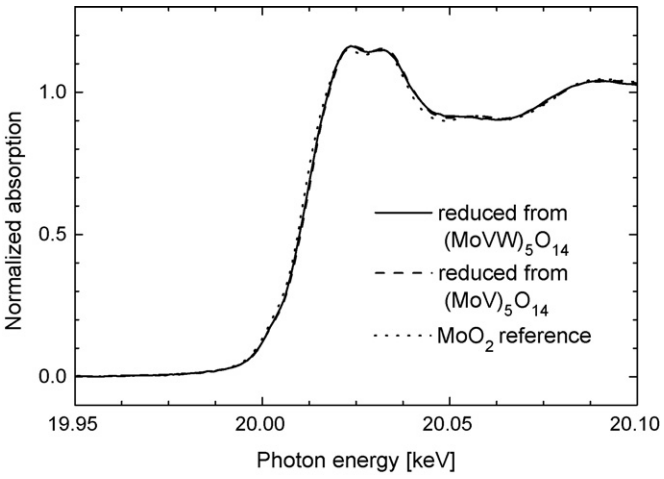

Fig. 5. XANES spectra of (MoVW) oxide and (MoV) oxide at the Mo K edge after reduction in 10% propene compared to a MoO_2 reference.

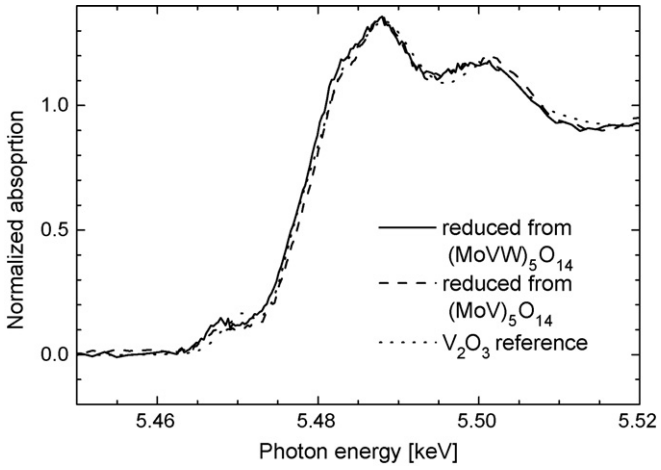

Fig. 6. XANES spectra of (MoVW) oxide and (MoV) oxide at the V K edge after reduction in 10% propene compared to a V_2O_3 reference.

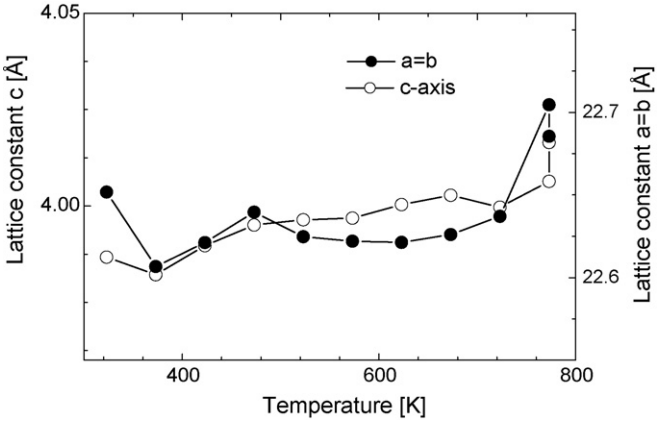

Fig. 7. Thermal expansion of lattice constants in $(MoVW)_5O_{14}$ during in situ XRD catalytic test in 5% propene and 10% oxygen.

720 K. The *a*/*b*-axis ($a = b$, tetragonal lattice) expand ca. 0.1–0.4% and the *c*-axis expands ca. 0.5% over the investigated temperature range. In $(MoV)_5O_{14}$ the observed lattice expansion occurred anisotropically in *a*/*b*- and *c*-direction (Fig. 8). The *c*-axis increases linear with temperature whereas

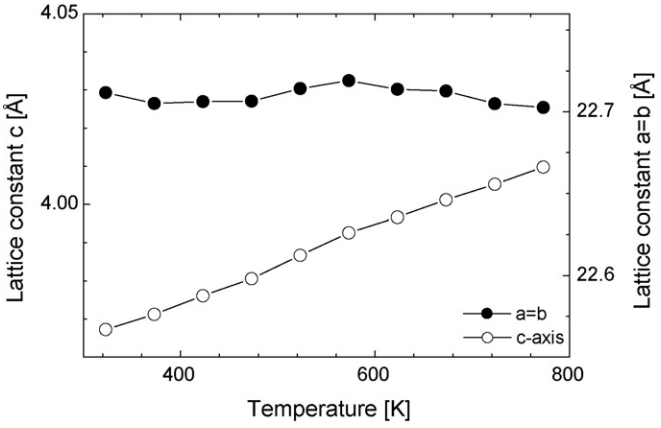

Fig. 8. Thermal expansion of lattice constants in $(MoV)_5O_{14}$ during in situ XRD catalytic test in 5% propene and 10% oxygen.

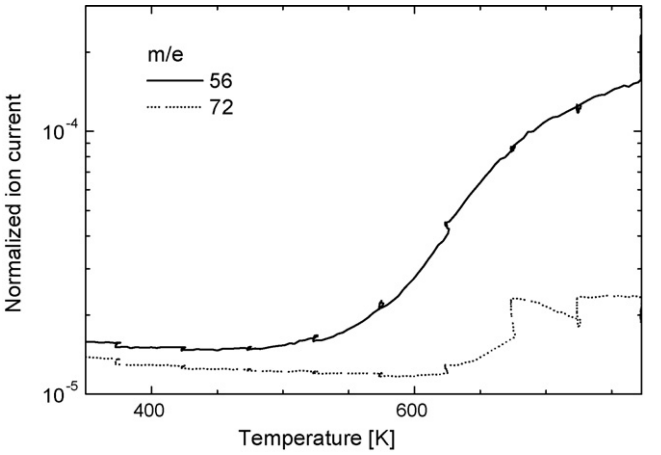

Fig. 9. Formation of acrolein ($m/e = 56$) and acrylic acid ($m/e = 72$) on $(MoVW)_5O_{14}$ during in situ XRD catalytic test in 5% propene and 10% oxygen.

for the *a*/*b*-axis an intermediate expansion with maximum elongation at 573 K is observed.

The formation of acrolein ($m/e = 56$) and acrylic acid ($m/e = 72$) during in situ XRD experiments is shown in Figs. 9 and 10, respectively. Products of selective oxidation were observed at temperatures higher than 550 K. Acrolein was detected on $(MoVW)_5O_{14}$ as well as on $(MoV)_5O_{14}$. The formation of acrylic acid was only detected on $(MoVW)_5O_{14}$.

4. Discussion

4.1. Influence of vanadium on electronic and geometric structure

Partially reduced vanadium centers in selective oxidation catalysts are assumed to enhance the hydrogen abstraction from hydrocarbon reactants. Accordingly, in the Mo_5O_{14}-type metal oxides investigated, the V centers exhibit an average valence of less than 5 (Fig. 3). During thermal treatment under reducing conditions, the V centers are reduced prior to the Mo or W centers. This may be in agreement with a participation of the V

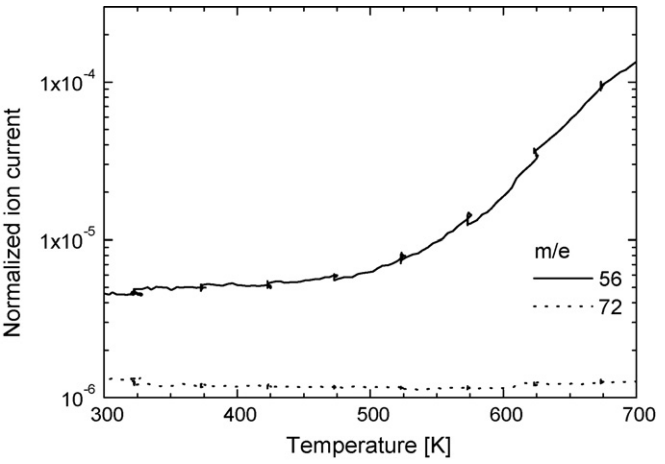

Fig. 10. Formation of acrolein ($m/e = 56$) on $(MoV)_5O_{14}$ during in situ XRD catalytic test in 5% propene and 10% oxygen.

centers in the active site of Mo_5O_{14}-type catalysts for selective oxidation. Conversely, the W centers in the mixed oxide catalysts may rather play a structural role than being involved in the catalytic cycle. The (MoVW) dioxide and (MoV) dioxide obtained from reduction of the Mo_5O_{14}-type materials exhibit a reduced average valence of the V centers (Fig. 6) compared the Mo centers (Fig. 5). This is in agreement with previous reports on the average valence of V centers in vanadium oxides doped with up to 10% molybdenum [22]. There, the authors did not detect changes in the Mo average valence but reduction of vanadium to preserve electro neutrality of the materials.

The long-range structural data presented indicate an influence of the V centers on the geometric structure of the Mo_5O_{14}-type materials studied. $(MoVW)_5O_{14}$ and $(MoV)_5O_{14}$ were prepared with different amounts of vanadium (i.e. 23% and 9%). Accordingly, a decrease in the lattice constants (Table 1) and the volume of the unit cell was found with an increasing V content (Fig. 11). Moreover, the distortion of the dioxide phases obtained from reduction of the Mo_5O_{14}-type materials from the nearly rutile type MoO_2 also increases with increasing V content (Table 2). In agreement with Vegard's law, the smaller size of the vanadium centers compared to Mo and W results in a reduced unit cell volume of the mixed oxides. Hence, (MoVW) dioxide possesses a smaller unit cell volume than (MoV) dioxide.

4.2. Stabilizing effect of tungsten in Mo_5O_{14}-type structures

$(MoV)_5O_{14}$ and $(MoVW)_5O_{14}$ were transformed into a monoclinic MoO_2-type phase (Figs. 1 and 2) during thermal treatment under reducing conditions (10% propene) at about 670 and 720 K, respectively. During treatment under oxidizing conditions (20% oxygen), the Mo_5O_{14}-type structure of $(MoVW)_5O_{14}$ was stable at 773 K. Conversely, the $(MoV)_5O_{14}$ material slowly undergoes a phase transformation into MoO_3-type material starting at 723 K. Apparently, the $(MoVW)_5O_{14}$ material exhibited a higher stability under reducing and oxidizing conditions compared to the tungsten-free $(MoV)_5O_{14}$ material. The onset temperature of the transformation of $(MoV)_5O_{14}$ into the MoO_3-type structure in oxygen is close to the onset temperature of the reduction of $(MoV)_5O_{14}$ in propene. The oxygen mobility in the oxide materials is a prerequisite for both, reduction to the MoO_2-type phase and oxidation to the MoO_3-type phase. On the other hand, tungsten in the $(MoVW)_5O_{14}$ material stabilizes the Mo_5O_{14}-type structure and prevents complete oxidation, even under conditions of sufficient oxygen mobility and a high oxidation potential of the gas phase.

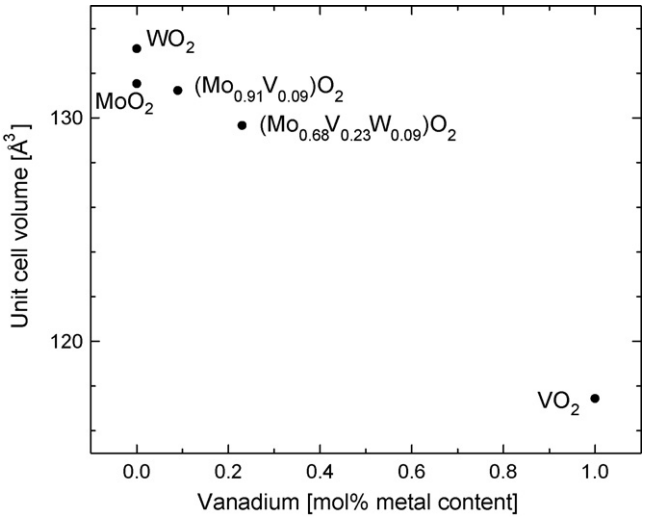

Fig. 11. Unit cell volume of metal oxides reduced in propene as a function of vanadium content for (MoVW) dioxide, (MoV) dioxide and binary oxides as reference compounds.

The stabilizing and structure directing effect of tungsten in the (MoVW) oxide is particularly apparent in the re-oxidation behavior of the corresponding (MoVW) dioxide. The tungsten centers in the MoO_2-type material obtained from reducing $(MoVW)_5O_{14}$ exert a strong structure-directing effect under oxidizing conditions. Re-oxidation of the (MoVW) dioxide leads to the re-formation of the Mo_5O_{14} structure. It has been frequently reported, that the Mo_5O_{14}-type structure can be obtained from thermal treatment of suitable molecular mixed metal precursors [14]. The corresponding reaction proceeds through a series of polycondensation steps resulting in the three-dimensional Mo_5O_{14} structure. Here we have shown for the first time that it is possible to transform the tetragonal $(MoVW)_5O_{14}$ material into a monoclinic MoO_2-type structure, and to then re-oxidize the (MoVW) dioxide into the Mo_5O_{14}-type structure. This striking ability is most likely due to the single cation position in the monoclinic structure which does not provide a driving force for further cation rearrangement.

Similar to our $(MoVW)_5O_{14}$ material, the reduction and re-oxidation properties of a $(MoVNb)_5O_{14}$ system as a suitable model catalyst have been recently discussed [23]. The $(MoVW)_5O_{14}$ material studied here combines suitable redox properties with a sufficient catalytic performance [24]. Therefore, it can be used as a model system for the redox behavior of the more complex MoVTeNb oxides applied in the selective oxidation of propane.

4.3. Catalysis of Mo_5O_{14}-type materials

The well crystalline materials show catalytic activity in the selective oxidation of propene. The long-range order of $(MoVW)_5O_{14}$ and $(MoV)_5O_{14}$ were stable under reaction conditions. The same holds for the short-range order or changes in the oxidation state of the metals involved.

Remarkably, $(MoVW)_5O_{14}$ and $(MoV)_5O_{14}$ show different selectivities in propene oxidation. Over $(MoVW)_5O_{14}$ the formation of both, acrolein and acrylic acid has been observed (Fig. 9). Conversely, only the formation of acrolein was detected on $(MoV)_5O_{14}$ (Fig. 10). This appears to be in contrast to previous reports [25–30] that have shown the formation of acrylic acid on MoV oxides, albeit, no single phase Mo_5O_{14}-type structured materials were studied in these investigations. The reaction conditions used (e.g. reactor geometry, space velocity) make comparisons with the cited references difficult. Indeed, the formation of traces of acrylic acid cannot be

excluded on $(MoV)_5O_{14}$. Incomplete analysis might be attributed to adsorption of acrylic acid on the walls of the reactor or the detection limit of the mass spectrometer. In any case, the formation of acrylic acid is certainly much higher on $(MoVW)_5O_{14}$ than on $(MoV)_5O_{14}$.

In both samples, $(MoVW)_5O_{14}$ and $(MoV)_5O_{14}$, the only crystalline phase detectable by XRD is the Mo_5O_{14}-type structure which was stable under reaction conditions. Therefore, the different product distribution cannot be attributed to bulk structural differences. Consequently, the differences of $(MoVW)_5O_{14}$ and $(MoV)_5O_{14}$ are mainly related to the chemical composition, i.e. the presence or absence of tungsten and the amount of vanadium (23% and 9%, respectively).

Still, the different bulk properties observed on the two samples and their different catalytic performance can be discussed with respect to surface relevance. Considering the concept of a particular active site, it requires a specific ensemble of metal atoms at the surface. The local structure of the active site is more likely to be formed at the surface if the corresponding bulk structure contains a similar structural motif. Apparently, compared to $(MoVW)_5O_{14}$, the inappropriate chemical composition and/or metal center ordering of the $(MoV)_5O_{14}$ surface gives rise to the different catalytic performance. In addition, the redox-stability of $(MoVW)_5O_{14}$ has to be considered. In the course of one catalytic cycle oxygen from the metal oxide surface is inserted into the hydrocarbon and the surface is reduced. Eventually, re-oxidation of the specific metal ensemble at the surface closes the catalytic cycle. The higher redox-stability of $(MoVW)_5O_{14}$ compared to $(MoV)_5O_{14}$ may lead to an improved structural recovery of the specific surface structure and thus, a superior catalytic performance of $(MoVW)_5O_{14}$.

5. Summary

Bulk structural properties and stabilities of crystalline single phase $(Mo_{0.91}V_{0.09})_5O_{14}$ and $(Mo_{0.68}V_{0.23}W_{0.09})_5O_{14}$ phases were investigated under reducing and oxidizing reaction conditions. A stabilizing effect of tungsten in the $(MoVW)_5O_{14}$ sample under oxidizing conditions was found. Additionally, tungsten centers in a (MoVW) dioxide material obtained from reducing $(MoVW)_5O_{14}$ exert a pronounced structure-directing effect under re-oxidation conditions. The effect of tungsten centers on the particular bulk structural properties of $(MoVW)_5O_{14}$ may account for the structural promoting effect of tungsten in selective oxidation.

Acknowledgement

HASYLAB/Hamburg is acknowledged for providing beamtime for this work. Dr. Di Wang is greatful acknowledged for TEM investigations.

References

[1] G. Mestl, Ch. Linsmeier, R. Gottschall, M. Dieterle, J. Find, D. Herein, J. Jäger, Y. Uchida, R. Schlögl, J. Mol. Catal. A: Chem. 162 (2000) 463.
[2] M. Dieterle, G. Mestl, J. Jäger, Y. Uchida, H. Hibst, R. Schlögl, J. Mol. Catal. A: Chem. 174 (2001) 169.
[3] S. Breiter, M. Estenfelder, H.-G. Lintz, A. Tenten, H. Hibst, Appl. Catal. A 134 (1996) 81.
[4] O. Ovsitser, Y. Uchida, G. Mestl, G. Weinberg, A. Blume, J. Jäger, M. Dieterle, H. Hibst, R. Schlögl, J. Mol. Catal. A 185 (2002) 291.
[5] V.M. Bondareva, T.V. Andrushkevich, G.I. Aleshina, L.M. Plyasova, L.S. Dovlitova, O.B. Lapina, D.F. Khabibulin, A.A. Vlasov, React. Kinet. Catal. Lett. 87 (2) (2006) 377.
[6] P. De Santo, D.J. Buttrey, R.K. Graselli, C.G. Lugmair, A.F. Volpe, B.H. Toby, T. Vogt, Top. Catal. 23 (2003) 1–4.
[7] L. Kihlborg, Arkiv Kemi 21 (40) (1963) 427.
[8] N. Yamazoe, L. Kihlborg, Acta Cryst. B 31 (1975) 1666.
[9] T. Ekström, M. Nygren, Acta Chem. Scand. 26 (1972) 1827.
[10] T. Ekström, Acta Chem. Scand. 26 (1972) 1843.
[11] T. Ekström, Mater. Res. Bull. 7 (1972) 19.
[12] T. Ekström, M. Nygren, Acta Chem. Scand. 26 (5) (1972) 1836.
[13] L. Kihlborg, Acta Chem. Scand. 23 (1969) 1834.
[14] S. Knobl, G.A. Zenkovets, G.N. Kryukova, O. Ovsitser, D. Niemeyer, R. Schlögl, G. Mestl, J. Catal. 215 (2003) 177.
[15] DIFFRAC plus Evaluation Package release, 2003.
[16] TOPAS Version 2.1 Bruker AXS.
[17] Inorganic Crystal Structure Database, Fachinformationszentrum (FIZ) Karlsruhe, Germany.
[18] T. Ressler, J. Synchrotron Rad. 5 (1998) 118.
[19] J. Wong, F.W. Lytle, R.P. Messmer, D.H. Maylotte, Phys. Rev. B 30 (10) (1984) 5596.
[20] T. Ressler, J. Wienold, R.E. Jentoft, T. Neisius, J. Catal. 210 (2002) 67.
[21] E. Rödel, R. Schlögl, T. Ressler, in preparation.
[22] F. Haaß, A.H. Adams, T. Buhrmester, G. Schimanke, M. Martin, H. Fuess, PCCP 5 (2003) 4317.
[23] M. Roussel, M. Bouchard, E. Bordes-Richard, K. Karim, S. Al-Sayari, Catal. Today 99 (1–2) (2005) 77.
[24] E. Rödel, S. Knobl, R. Schlögl, T. Ressler, in preparation.
[25] A.H. Adams, F. Haaß, T. Buhrmester, J. Kunert, J. Ott, H. Vogel, H. Fuess, J. Mol. Catal. A 216 (1) (2004) 67.
[26] J. Kunert, A. Drochner, J. Ott, H. Vogel, H. Fuess, Appl. Catal. A 269 (2004) 53.
[27] K. Krauß, A. Drochner, M. Fehlings, J. Kunert, H. Vogel, J. Mol. Catal. A 162 (2000) 413.
[28] K. Krauß, A. Drochner, M. Fehlings, J. Kunert, H. Vogel, J. Mol. Catal. A 177 (2002) 237.
[29] T.V. Andrushkevich, Catal. Rev.-Sci. Eng. 35 (2) (1993) 213.
[30] H. Vogel, R. Böhling, H. Hibst, Catal. Lett. 62 (1999) 71.